HHS Public Access

Author manuscript

Nat Med. Author manuscript; available in PMC 2017 May 05.

Published in final edited form as:

Nat Med. 2015 September ; 21(9): 1076–1084. doi:10.1038/nm.3925.

A novel mechanism of cardioprotection through TNF-α-induced ectopic expression of keratins K8 and K18

Stamatis Papathanasiou[1], **Steffen Rickelt**[2,#], **Mageni Soriano**[3], **Tobias Schips**[4], **Harald J. Maier**[5], **Constantinos H. Davos**[6], **Aimilia Varela**[6], **Loukas Kaklamanis**[7], **Luca Scorrano**[3], **Douglas L. Mann**[8], and **Yassemi Capetanaki**[1]

[1]Center of Basic Research, Biomedical Research Foundation of Academy of Athens, 11527 Athens, Greece

[2]Helmholtz Group for Cell Biology, German Cancer Research Center, Im Neuenheimer Feld 581, D-69120-Heidelberg, Germany

[3]Department of Biology, University of Padua, Viale G. Colombo 3, 35121 Padova, Italy

[4]Department of Pediatrics, Cincinnati Children's Hospital Medical Center, Cincinnati, 45229 Ohio, USA

[5]Institute of Physiological Chemistry, University of Ulm, Albert-Einstein-Allee 11, 89081 Ulm, Germany

[6]Center of Clinical Research, Biomedical Research Foundation of Academy of Athens, 11527 Athens, Greece

[7]Onassis Cardiac Surgery Center, 17674 Athens, Greece

[8]Center of Cardiovascular Research, Division of Cardiology, Department of Medicine, Washington University School of Medicine, St Louis, 63110 MO, USA

Abstract

The adult myocardium demonstrates a unique system of adaptation upon stress stimuli, in an effort to maintain its overall homeostasis. This compensatory mechanism remains a mystery[1]. Tumor Necrosis Factor-α (TNF-α) is one of the major stress-induced pro-inflammatory cytokines that is up-regulated in heart failure[1,2] and its sustained expression is considered detrimental for the heart[1,3–9]. Although previous studies have shown that lower levels of TNF-α confer cytoprotection in the myocardium following ischemic reperfusion injury[10], such action in heart failure remains elusive. Here we propose a novel cardioprotective function for TNF-α overexpression in a genetic heart failure model, the desmin deficient mice, through NF-κB-mediated cardiomyocyte ectopic

Correspondence should be addressed to YC (ycapetanaki@bioacademy.gr).

[#]David H. Koch Institute for Integrative Cancer Research, Massachusetts Institute of Technology, Cambridge, 02139 MA, USA (present address)

Author contribution

Y.C. and S.P. conceived the project, designed research and analysed all the data; S.P. performed the research, S.R. helped with the EM experiments. M.S. and L.S. helped with the mitochondrial functional experiments. T.S. helped with the experiments on several models of HF. C.H.D. and A.V. helped with echocardiography. H.J.M. contributed with analyses of the IKK^{MyHC} mice., L.K. provided the human samples, D.L.M. provided the original MHCsTNFα mice, helped with TAC experiments and data interpretation. S.P. and Y.C. wrote the paper and Y.C. supervised all aspects of the work. All co-authors approved the manuscript submitted.

expression of keratin 8 (K8) and keratin 18 (K18)[11], two simple epithelia-specific Intermediate Filament (IF) proteins. The ectopically expressed K8 and K18 (K8/K18) form a cytoskeletal network that localizes mainly at the Intercalated Discs (IDs). This alternative K8/K18 cytoskeleton confers cardioprotection by a mechanism that maintains ID and mitochondrial integrity and function. Importantly, we demonstrated that K8/K18 ectopic induction takes place in other genetic and experimental models of heart failure and showed a cardioprotective function in mice subjected to transverse aortic constriction. Finally, we discovered that in cardiomyocytes of human failing myocardium, where TNF-α is induced[2], K8/K18 are also ectopically expressed and localize primarily at IDs, where desmin cannot be detected. This is the first report to propose a TNFα-mediated cardiac ectopic expression of K8/K18 IF proteins, which may act as stress-induced cardioprotective factors in the failing heart, a phenomenon of major clinical significance as it also extends to human heart failure.

The role of the pleiotropic intercellular cytokine TNF-α in the heart pathophysiology has been considerably debated in the scientific community[12]. Although it is not constitutively expressed in the heart[13,14], it is rapidly and consistently expressed in response to various forms of myocardial injury as part of an intrinsic cardiac response system[1].

Accumulating data from various models established that TNF-α engenders deleterious effects in the myocardial structure and function, which mimic the characteristic phenotype of heart failure[1,3–9]. On the other hand, little is known about the possible beneficial effects of TNF-α in the heart[10,15–17], while its potential cardioprotective mechanisms remain elusive. Uncovering the mechanisms of TNF-α-mediated cardioprotection, may explain the failure of anti-TNF-α clinical trials[18] and allow the development of more efficient therapeutic approaches for human heart failure.

A critical step towards the delineation of TNF-α action in the myocardium, emerged from our recent study using the “MHCsTNFα” mice[3] (myosin heavy chain promoter-driven cardiac-specific overexpression of TNF-α, hereafter named “TNF-α” mice), in which the TNF-α-mediated detrimental effects had been well demonstrated[3,5,19,20]. We showed that desmin, the muscle-specific IF protein, is a major target in TNFα-induced cardiomyopathy[21,22]. Specifically, desmin is cleaved by TNF-α-induced caspase-6, loses its proper ID localization and forms aggregates. In TNF-α mice expressing a caspase cleavage-resistant desmin mutant (D263E), cardiac myocyte apoptosis was attenuated, left ventricular (LV) wall thinning was prevented and cardiac function was improved, thus revealing an important role for desmin cleavage in the development of dilated cardiomyopathy and heart failure.

The clinical significance of desmin has been demonstrated by the discovery of a plethora of mutations in the *desmin* gene that have been associated with desmin-related myopathies[22,23]. A milestone towards understanding the significance of the IF cytoskeleton in the myocardium was the generation of desmin-deficient (Des−/−) mice[24,25], a widely established model of Dilated Cardiomyopathy (DCM) and heart failure, characterized by myocardial necrosis, early inflammation and extensive fibrosis and calcification[24,26].

Surprisingly, crossing TNF-α and Des−/− mice, two known heart failure models, results in a considerable rescue of the typical Des−/− extensive myocardial degeneration. Extensive fibrotic lesions (characterized as “replacement fibrosis”) and calcified areas, characteristic of Des−/− pathology[24,26], are totally absent in TNFαDes−/− myocardium (Fig. 1a). There is also a marked reduction of ventricular wall thinning and dilation (Fig. 1a), further verified by echocardiographic analysis (Supplementary Fig. 1b–c and Table 1). The typical myocardial necrosis and inflammation are significantly attenuated in TNFαDes−/− littermates (Fig. 1b and Supplementary Figs 2 and 3). Cardiomyocyte ultrastructural defects, particularly in mitochondrial morphology and distribution and secondarily in myofibril integrity, are hallmarks of the desmin-deficient cardiomyopathy[27]. Transmission electron microscopy of both cardiac sections as well as isolated mitochondria demonstrated that the overall ultrastructure of TNFαDes−/− cardiomyocytes is significantly improved compared to Des−/− myocardium (Fig. 1c, 1e and Supplementary Fig. 4e–f). Specifically, the aberrant matrix fragmentation and abnormal cristae remodeling characteristic of Des−/− mitochondria[27] decrease extensively in TNFαDes−/− mitochondrial preparations. (Fig. 1e and Supplementary Fig. 5e). Furthermore, the overall cardiac mitochondrial function which is compromised in Des−/− heart is extensively rescued upon TNF-α overexpression. Specifically, the prominent decrease of Des−/− mitochondrial respiratory function, as estimated by measuring oxygen consumption (respiratory control ratio, State-III/State-IV) (Fig. 1d and Supplementary Fig. 5a) in isolated mitochondria of 3-mo-old hearts, was significantly improved in TNFαDes−/− hearts. This finding was in agreement with extensive rescue in TNFαDes−/− hearts of ATP production levels (Supplementary Fig. 5b) and redox activities, as measured by analysis of the reduction efficiency of GSSG and $NADP^+$ to GSH and NADPH respectively (Supplementary Fig. 5c–d). Furthermore, this unexpected fundamental attenuation of heart abnormalities in TNFαDes−/− mice is further reflected to significant improvement of physiological cardiac functional properties, like fractional shortening (FS) (TNFαDes−/− vs Des−/−: 37.69% vs 34.63% at 3-mo-old and 35.73% vs 27.03% at 6-mo-old mice respectively; p-value<0.001) (Fig. 1f, Supplementary Fig. 1 and Table 1).

In an effort to further understand the mechanism by which TNF-α rescues the Des−/− myocardium, we analyzed the transcriptome changes in TNFαDes−/− relative to Des−/− hearts, by whole genome microarray analysis. Among 646 genes with significantly altered expression (FC≥±2, p-value≤0.05) in TNFαDes−/− heart, 206 are down-regulated and 440 up-regulated (Supplementary Fig. 3). Data meta-analysis revealed that the up-regulated genes (FC≥2) are mainly implicated in ‘cell death’ and ‘cell-to-cell signaling and interaction’ responses (Supplementary Fig. 3c). On the other hand, the most prominent down-regulation is observed in genes associated with inflammation/immunity and tissue remodelling related processes (Supplementary Fig. 4c, Table 2 and Data Set 1), reflecting the absence of leukocyte infiltration and inflammation in TNFαDes−/− hearts (Supplementary Fig. 2), in contrast to Des−/− hearts[26],.

Interestingly, among the most pronounced and surprising changes was the high-level ectopic induction of *krt8* and *krt18* genes, encoding for the epithelial intermediate filament proteins, keratin 8 (K8) and keratin 18 (K18) (16.44 and 25.96 fold increase respectively in TNFαDes −/− vs Des−/− hearts; see Fig. 2a and Supplementary Table 2). K8 and K18 are normally

expressed in the simple epithelium of various organs (such as liver, kidney, mammary gland etc.)[11] and have never been detected in the adult myocardium or in other muscle types, following the known strictly regulated tissue-specific pattern of IF proteins[11,28,29]. However, very low expression of another keratin pair, K8/K19, has been reported in striated muscle[30]. Real-Time PCR analysis confirmed the high levels of ectopic *krt8* and *krt18* RNA expression in TNFαDes−/− hearts (53.2 and 62.7 fold increase, respectively, in TNFαDes−/− vs WT) and further established that this induction takes place in TNF-α (Des+/+) hearts as well (Fig. 2b). The expression of the *krt8* and *krt18* genes was also confirmed at the protein level (Fig. 2c). Furthermore, we showed by immunofluorescence microscopy that K8/K18 are expressed throughout the myocardial area in TNFα-overexpressing mice (Fig. 2i). This expression pattern is evident in the hearts from neonatal (Supplementary Fig. 6) till aged TNFαDes−/− mice and persists at all age groups studied (data not shown). Control WT myocardium was always negative for K8/K18, both by western (Fig. 2c) and immunofluorescence microscopy analysis (Fig. 2i), as expected from previous studies[11,28,29]. Intriguingly, in Des−/− myocardium K8/K18 expression is detectable, although less evident and in scattered islets of cardiomyocytes (Supplementary Fig. 7).

To address the mechanism of the K8/K18 ectopic induction in TNFαDes−/− myocardium, we explored the potential involvement of Nuclear Factor-κB (NF-κB), known to be activated by TNF-α, on the transcriptional induction of both *krt8* and *krt18* genes. Due to very limited information on *krt8* and *krt18* gene regulation, a bioinformatics analysis (including ENCODE Consortium data and transcription factor binding sites prediction tool, Supplementary Tables 3 and 4) was performed, which revealed several potential regulatory regions in *krt8*/*krt18* loci (Supplementary Fig. 8). Following *in vivo* cardiac chromatin immunoprecipitation experiments for the p65/RelA subunit of NF-κB, these regions were used as targets for RT-PCR enrichment of the precipitated chromatin fragments. Our data imply that NF-κB is involved in the ectopic activation of both *krt8* and *krt18* gene transcription in TNFαDes−/− heart, by binding to at least one genomic regulatory locus of each gene (K8R2P1 region for *krt8,* K18R1P3 and K18R2P2 regions for *krt18*) and to an intergenic region of potential regulation (K8K18R2P2) (Fig 2d and Supplementary Fig. 8).

The NF-κB involvement in the ectopic induction of K8/K18 in the heart was further verified using an *in vivo* model of cardiac-specific transgenic expression of constitutively active IKK2 (IKK^{MyHC} mice), the kinase responsible for canonical NF-κB activation[31]. Indeed, in contrast to control group, IKK^{MyHC} mice showed ectopic expression of K8/K18 in the myocardium (Fig. 2e–f and Supplementary Fig. 9a–b). Induction was evident both before (5-weeks of doxycycline withdrawal) and after (12-weeks of doxycycline withdrawal) manifestation of an overt heart failure phenotype, which in these mice usually starts to develop 6- to 8-weeks post doxycycline discontinuation[31]. Furthermore, complementary to the IKK^{MyHC} gain-of-function *in vivo* model, a ‘loss-of-function’ *in vivo* approach was also utilized to verify the NF-κB involvement in K8/K18 ectopic induction in the heart. Crossing the TNF-α mice with a model of NF-κB signaling blockade, conferred by cardiac-specific expression of an IκBa superreppressor (IκBα-3M mice)[32], resulted in a significant decrease of both *krt8* and *krt18* ectopic expression in the heart (29% and 41% respectively, p-value<0.05)(Fig 2g).

Reporter assays also verified the *in vivo* data on the involvement of NF-κB in the transcriptional regulation of *krt8* and *krt18*. By using a realistic system of a 2-kb-long genomic region upstream of their translation start sites (see Supplementary Fig. 9c), thus including all the regulatory loci, as described in Supplementary Figure 8, we showed that both *krt8* and *krt18* are significantly responsive to p65 induction (1.91 and 2.08 respectively, fold change relative to non-induced, p-value<0.001)(Fig. 2h). Furthermore, mutations on the specific κB-sites found to bind p65 *in vivo* (Fig. 2d and Supplementary Fig.8), were adequate to significantly reduce the p65-dependent *krt8* and *krt18* induction (23% and 40% respectively, relative to WT-induced, p-value<0.05)(Fig. 2h and Supplementary Fig. 9e). The effect of the specific κB-site mutations on the *krt8* and *krt18* regulation was also observed under baseline conditions (Supplementary Fig. 9d–e).

Using immunofluorescence microscopy, we demonstrated that the ectopic expression of both K8/K18 proteins in TNF-overexpressing hearts is restricted to cardiomyocytes, where they fully co-localize (Fig. 2j), while they cannot be detected in cardiac fibroblasts (Supplementary Fig. 10). The 'area composita' (fusion of desmosomes and *fasciae adherente*)[33] of the intercalated discs (IDs) is the major localization site of the K8/K18 pair in TNFαDes−/− cardiomyocytes (Figs 2j–k and Supplementary Fig. 4a). Similarly to desmin in normal myocardium, K8/K18 co-localize with major components of desmosomes and adherens junctions, such as desmoplakin (DSP) and β-catenin (β-cat) respectively, at the IDs of TNFαDes−/− myocardium (Fig. 2k and Supplementary Fig. 4a). Z-disc localization was not detected, however, a sarcoplasmic striated pattern of K8/K18 at the M-line level of the myofibrils extending to the costameres could be observed (Fig. 2j and Supplementary Fig. 4b). Immunoelectron microscopy further confirmed the keratin 8 specificity for the cardiomyocyte ID plaques and allowed the detection of the filamentous organization of the ectopic K8/K18 network (Fig. 2l and Supplementary Fig. 4c).

Keratins have been linked to several mechanical and non-mechanical cytoprotective functions[34–40]. Notably, K8/K18 have been involved in several diseases, from liver pathophysiology to cancer, in modulation of signal transduction pathways, protection from cell death, protein targeting and organelle regulation and transport[34–37,39–43]. Therefore, we asked whether the highly expressed and specifically localized K8/K18 in TNFαDes−/− cardiomyocytes could be responsible for the TNF-α-mediated rescue of the myocardial degeneration and dilated phenotype observed in the Des−/− mice. To address this issue, we generated TNFαDes−/−Krt18−/− mice, which provide a K8/K18 deficient model, given that keratin 8 is degraded in the absence of its partner[41].

While gross morphology of TNFαDes−/−Krt18−/− hearts appears similar to those from TNFαDes−/− mice, histological sections reveal a more prominent dilated phenotype (Fig. 3a), and this is further verified by echocardiographic analysis (Supplementary Fig. 1 and Table 1). Additionally, interstitial fibrosis appears to be increased in TNFαDes−/−Krt18−/− hearts and areas of replacement fibrosis are occasionally evident (Fig. 3a´), in contrast to TNFαDes−/− myocardium. Echocardiographic data prove that the TNF-α-mediated cytoprotective action is lost in the absence of K8/K18, manifested by a significant reduction in the overall cardiac function in TNFαDes−/−Krt18−/− compared to TNFαDes−/− mice (FS: 31.64% vs 37.69% at 3-mo-old and 27.68% vs 35.73% at 6-mo-old respectively; p-

value<0.0001) (Fig. 3b, Supplementary Fig. 1 and Table 1). While the worse pathophysiology of TNFαDes−/−Krt18−/− hearts clearly demonstrates the K8/K18 cardioprotective effect, in the TNFαKrt18−/− myocardium such an effect is not profound. No significant changes in fractional shortening (Supplementary Table 1) and histology (data not shown) compared to TNF-α mice, are observed, consistent with the known dominant effect of the defective desmin network in this model[21]. However, lack of K8/K18 leads to a more dilated phenotype in TNFαKrt18−/− mice (Supplementary Fig. 1 and Table 1), demonstrating a cardioprotective effect of K8/K18 in TNF-α model as well. Krt18−/− control mice appear similar to WT by morphological, histological and echocardiographic analysis (Figs 3a–b), while the Des−/−Krt18−/− myocardium demonstrates similar to Des−/− pathologic characteristics, including extensive replacement fibrosis, calcification and myocardial degeneration (data not shown).

One of the important functional roles of K8/K18 stems from their interaction with desmosomes, the intercellular adhesive junctions of epithelial cells. This critical interaction confers stabilization and maintenance of the desmosome structures[44], proper targeting of desmosomal proteins[43], subsequent maintenance of surface membrane integrity[45] and facilitation of intercellular mechanical and ionic communication[45,46]. Complementary to protein targeting function, another important role of IFs is organelle modulation, specifically that of mitochondria[27,37,47–49]. Evidence for the importance of IF cytoskeleton in mitochondrial structure and function was provided by previous studies in Des−/− mice[27,50], supporting the data of Figure 1. Additionally, recent data suggest a similar cytoprotective mechanism of K8/K18 (or K8/K19) at the mitochondrial level[42,49,51,52]. Therefore, we hypothesized that the mechanism of protection by K8/K18 in TNFαDes−/− mice could be through maintenance of mitochondrial, ID and myofibril integrity.

Electron microscopy studies revealed that the TNFαDes−/−Krt18−/− myocardium presents severe ultrastructural defects. Mitochondria accumulate and aggregate atypically and are disarranged (Fig. 3c and Supplementary Fig. 11a), while myofibril organization is also defective, compared to TNFαDes−/− myocardium (Fig. 3c and Supplementary Fig. 4e–f). Mitochondrial abnormalities resemble the characteristic defects in desmin-deficient cardiomyopathy[47], reflecting a central role of IFs in mitochondrial homeostasis and suggesting that K8/K18 can compensate for proper mitochondria regulation in the absence of desmin. Indeed, partially or totally swollen mitochondria (“phase-III” and “phase-IV”, see Supplementary Fig. 5 legend) are prominent in TNFαDes−/−Krt18−/− hearts (Fig. 3c and Supplementary Fig. 5e). Importantly, the ultrastructural abnormalities also reflect a significant impairment of mitochondrial functional status in the absence of K8/K18 network, as their respiration is severely defective (Fig. 3d and Supplementary Fig. 5a). Furthermore, ATP levels (Supplementary Fig. 5b) and redox activities (Supplementary Fig. 5c–d) are abnormal compared to TNFαDes−/− cardiac mitochondria, similarly to Des−/−. These findings support a mitoprotective effect of K8/K18 network in TNFαDes−/− cardiomyocytes, as a mechanism of TNF-mediated cardioprotection in Des−/− myocardium.

Furthermore, the IDs of TNFαDes−/−Krt18−/− cardiomyocytes are severely abnormal, being discontinuous and amorphous compared to typical IDs of WT and TNFαDes−/− myocardium (arrowheads in Fig. 3f). Consistent with this finding is the mis-targeting of

critical components of the 'area composita', including Desmoplakin, Plakoglobin and β-Catenin in TNFαDes−/−Krt18−/− myocardium (Fig. 3e) and Supplementary Fig. 11b). This finding suggested that the proper targeting or maintenance of these proteins to IDs is part of the mechanism by which the K8/K18 network compensates for the desmin deficiency in TNFαDes−/− hearts.

A critical question raised by our findings was whether the K8/K18 expression in TNF-overexpressing mice reflects a common response in heart failure. To address this important issue we introduced additional, well established, genetic and experimental models of heart failure and investigated the *krt8* and *krt18* expression status in the heart. Importantly, we found that both these genes are ectopically induced in transgenic hearts with cardiac-specific overexpression of constitutively active Calcineurin (MHC-Cn)[53], a calcium-dependent phosphatase, and in muscle–specific LIM-only protein knockout (MLP−/−)[54] hearts (Fig. 4a´). Notably, they present the same protein localization properties described for TNF-overexpessing cardiomyocytes (Fig. 2j–k), in a significantly lower extent though, forming a network localized in the cardiomyocyte IDs and costameric striations (Fig. 4a´´–a´´´). Moreover, we showed that K8/K18 ectopic network is also evident in experimentally induced HF (Fig. 4b). Cardiomyocytes of WT mice subjected to either transverse aortic constriction (TAC) (Fig. 4b´–b´´ and Supplementary Fig. 12a–d) or myocardial infarction (MI) by permanent ligation of the left anterior descending (LAD) coronary artery, exhibit the characteristic pattern as discussed for the genetic models of HF. All appropriate WT control groups studied were never found positive for K8/K18 expression. These data provide strong evidence for a global nature of K8/K18 ectopic induction in stressed or failing cardiomyocytes.

An important finding supporting the cardioprotective effect of K8/K18 ectopic induction in the heart was provided using the TAC experimental model of HF. We demonstrated that mice deficient in K8/K18 network (Krt18−/−) exhibit very early, by two weeks post-TAC, a heart failure response, as their hearts show a significant decrease of 25.1% (Fig. 4c´ and Supplementary Table 5) in the fractional shortening compared to WT baseline levels (baseline FS: 52.21%; 2-weeks post-TAC FS: 39.09%) (Fig. 4c and Supplementary Fig. 12e and Table 5). Most possibly, this is due to failure of Krt18−/− hearts to compensate for the pressure overload stress in contrast to WT mice, given that they do not undergo the normal hypertrophic response observed in WT mice justified by a significant increase of relative wall thickness (RWT)(Fig. 4c´´). Instead, Krt18−/− hearts develop dilation as measured by a significant decrease in left ventricular dimensions in systole (LVIDs) (Supplementary Fig. 12e´), in contrast to WT. Consistent to the findings of Figure 4b, the WT TACed mice used in this study were found positive to K8/K18 network formation presenting the typical ID and striated pattern in cardiomyocytes (Fig. 4d and Supplementary Fig. 12a–d).

Finally, we set to answer the next important question about the relevance of our findings in human heart failure as well, where TNF-α has been shown to be up-regulated[2]. Using cardiac samples from patients that underwent heart transplantation, we demonstrated that, indeed, both keratin 8 and keratin 18 proteins are expressed in human failing heart, showing variable levels of K8 and K18 ectopic expression between the patients (Fig. 4e and Supplementary Fig. 13a). Serum TNF-α levels in the group of these patients were found

significantly increased compared to a normal group (Fig. 4f), as expected[2]. Similarly to our findings in murine models of HF, we found that K8 and K18 co-localize in the cardiomyocytes of the human failing myocardium (Fig. 4h´ and Supplementary Fig. 13c), supporting the clinical importance of our observations. Similarly to our studies with mice, K8/K18 expression occurs specifically in cardiomyocytes and not in cardiac fibroblasts (Fig. 4g and Supplementary Fig. 10b). Moreover, K8/K18 are clearly detected at the IDs where they co-localize with desmosomal (Fig. 4g) and adherens junction proteins (data not shown). No K8/K18 formation was detected in cardiomyocytes of normal human myocardium (Supplementary Fig. 13b), in agreement with the literature[11,28,29]. Thus, the significantly lower levels of K8/K18 detected by WB in control myocardium (Fig. 4e and Supplementary Fig. 13a) may correspond to non-cardiomyocyte cells of the epicardium or endothelial cells of the heart microvasculature[55].

Based on our previous data in mice[21], we also investigated the characteristics of desmin network in human heart failure. Importantly, we found that desmin is significantly accumulated in human failing myocardium in all cases tested (Fig. 4e). Desmin protein levels are elevated in the patient samples compared to healthy myocardium, most possibly due to lower degradation rate of aggregated desmin[21]. Furthermore, immunofluorescence microscopy revealed that, in agreement with our previous findings in mice[21], desmin loses extensively its proper ID localization (Fig. 4i). Notably, K8/K18 show more efficient ID localization compared to desmin (Fig. 4h´´ and Supplementary Fig. 13c´´), consistent with our data in TNF-α mice (Supplementary Fig. 14). This could be possibly related to the potential modification of desmin by caspase-6-mediated cleavage, as we had previously demonstrated in TNF-α failing myocardium[21]. Indeed, desmin-cleavage products are evident in some of the patient samples and not in control human myocardium (arrows in Fig. 4e). This is the first report of desmin cleavage and mis-localization in human end-stage heart failure, the latter abnormality reported before only in Carvajal Syndrome[56].

Collectively our results demonstrate a novel cardioprotective role for TNF-α through *de novo* expression of epithelial IF proteins in the heart. This is the first study to report a reprogramming mechanism by which this cytokine may contribute to overcoming restrictions required to maintain tissue-specific gene expression in adult cardiomyocytes, thus leading to keratin 8 and keratin 18 expression. These proteins form obligatory heteropolymers, a prerequisite for the generation of a properly functioning intermediate filament network[34]. Therefore, the potential of TNF-α to ectopically activate both genes through NF-κB plays a major role in the achieved cardioprotection. Furthermore, the ability of K8/K18 to maintain ID integrity and mitochondrial function strongly support the notion that this keratin network might be an ideal alternative IF cytoskeletal system to compensate for desmin deficiency.

These novel discoveries suggest the reconsideration of the present knowledge of myocardial biology and denote the need for re-evaluation of our current interpretation of mechanisms involved in heart pathophysiology, which could potentiate more effective therapeutic approaches in human heart disease. Furthermore, the potential diagnostic and even prognostic value of these findings for different types and stages of heart pathology is substantial and should be thoroughly investigated and clinically evaluated.

Supplementary Material

Refer to Web version on PubMed Central for supplementary material.

Acknowledgments

We thank very much Prof W. Franke and Y. Dörflinger from the Division of Cell Biology in German Cancer Research Center, for extensive technical support with EM and immunogold labelling, for providing materials and very valuable comments. We thank Prof W.K. Jones, University of Cincinnati, for kindly providing the IκBα-3M mice, M. Gerstenlauer, Institute of Physiological Chemistry, University of Ulm, for technical assistance with IKK^{MyHC} mice experiments and Prof. J. D. Molkentin, Howard Hughes Medical Institute and Cincinnati Children's Hospital Medical Center, for providing materials. We also thank P. Politis and N. Athanassiadis, Biomedical Research Foundation of Academy of Athens, for providing materials.

This work was supported by Greek Secretariat of Research and Development grants (PENED 01ED371, PEP-ATT-39, ESPA SYNERGASIA SYN 965) to YC and a fellowship (Heracleitus II) by the European Union and Greek national funds through the Operational Program "Education and Lifelong Learning" of the National Strategic Reference Framework to SP.

References

1. Mann DL. Stress-activated cytokines and the heart: from adaptation to maladaptation. Annual review of physiology. 2003; 65:81–101.
2. Levine B, Kalman J, Mayer L, Fillit HM, Packer M. Elevated circulating levels of tumor necrosis factor in severe chronic heart failure. The New England journal of medicine. 1990; 323:236–241. [PubMed: 2195340]
3. Li X, et al. Cardiac-specific overexpression of tumor necrosis factor-alpha causes oxidative stress and contractile dysfunction in mouse diaphragm. Circulation. 2000; 102:1690–1696. [PubMed: 11015349]
4. Finkel MS, et al. Negative inotropic effects of cytokines on the heart mediated by nitric oxide. Science (New York, N.Y. 1992; 257:387–389.
5. Sivasubramanian N, et al. Left ventricular remodeling in transgenic mice with cardiac restricted overexpression of tumor necrosis factor. Circulation. 2001; 104:826–831. [PubMed: 11502710]
6. Bozkurt B, et al. Pathophysiologically relevant concentrations of tumor necrosis factor-alpha promote progressive left ventricular dysfunction and remodeling in rats. Circulation. 1998; 97:1382–1391. [PubMed: 9577950]
7. Pagani FD, et al. Left ventricular systolic and diastolic dysfunction after infusion of tumor necrosis factor-alpha in conscious dogs. The Journal of clinical investigation. 1992; 90:389–398. [PubMed: 1644912]
8. Natanson C, et al. Endotoxin and tumor necrosis factor challenges in dogs simulate the cardiovascular profile of human septic shock. The Journal of experimental medicine. 1989; 169:823–832. [PubMed: 2647895]
9. Krown KA, et al. Tumor necrosis factor alpha-induced apoptosis in cardiac myocytes. Involvement of the sphingolipid signaling cascade in cardiac cell death. The Journal of clinical investigation. 1996; 98:2854–2865. [PubMed: 8981934]
10. Burchfield JS, et al. The cytoprotective effects of tumor necrosis factor are conveyed through tumor necrosis factor receptor-associated factor 2 in the heart. Circ Heart Fail. 2010; 3:157–164. [PubMed: 19880804]
11. Moll R, Franke WW, Schiller DL, Geiger B, Krepler R. The catalog of human cytokeratins: patterns of expression in normal epithelia, tumors and cultured cells. Cell. 1982; 31:11–24. [PubMed: 6186379]
12. Duran WN. The double-edge sword of TNF-alpha in ischemia-reperfusion injury. American journal of physiology. 2008; 295:H2221–H2222. [PubMed: 18849327]
13. Kapadia S, et al. Tumor necrosis factor-alpha gene and protein expression in adult feline myocardium after endotoxin administration. The Journal of clinical investigation. 1995; 96:1042–1052. [PubMed: 7635940]

14. Kapadia SR, et al. Elevated circulating levels of serum tumor necrosis factor-alpha in patients with hemodynamically significant pressure and volume overload. Journal of the American College of Cardiology. 2000; 36:208–212. [PubMed: 10898436]
15. Kurrelmeyer KM, et al. Endogenous tumor necrosis factor protects the adult cardiac myocyte against ischemic-induced apoptosis in a murine model of acute myocardial infarction. Proceedings of the National Academy of Sciences of the United States of America. 2000; 97:5456–5461. [PubMed: 10779546]
16. Lecour S, et al. Identification of a novel role for sphingolipid signaling in TNF alpha and ischemic preconditioning mediated cardioprotection. Journal of molecular and cellular cardiology. 2002; 34:509–518. [PubMed: 12056855]
17. Deuchar GA, Opie LH, Lecour S. TNFalpha is required to confer protection in an in vivo model of classical ischaemic preconditioning. Life sciences. 2007; 80:1686–1691. [PubMed: 17316703]
18. Feldman AM, Kadokami T, Higuichi Y, Ramani R, McTiernan CF. The role of anticytokine therapy in heart failure: recent lessons from preclinical and clinical trials? The Medical clinics of North America. 2003; 87:419–440. [PubMed: 12693732]
19. Haudek SB, Taffet GE, Schneider MD, Mann DL. TNF provokes cardiomyocyte apoptosis and cardiac remodeling through activation of multiple cell death pathways. The Journal of clinical investigation. 2007; 117:2692–2701. [PubMed: 17694177]
20. Engel D, Peshock R, Armstong RC, Sivasubramanian N, Mann DL. Cardiac myocyte apoptosis provokes adverse cardiac remodeling in transgenic mice with targeted TNF overexpression. American journal of physiology. 2004; 287:H1303–H1311. [PubMed: 15317679]
21. Panagopoulou P, et al. Desmin mediates TNF-alpha-induced aggregate formation and intercalated disk reorganization in heart failure. The Journal of cell biology. 2008; 181:761–775. [PubMed: 18519735]
22. Capetanaki Y, Papathanasiou S, Diokmetzidou A, Vatsellas G, M T. Desmin related disease: a matter of cell survival failure. Current opinion in cell biology. 2015; 32:113–120. [PubMed: 25680090]
23. Goldfarb LG, Dalakas MC. Tragedy in a heartbeat: malfunctioning desmin causes skeletal and cardiac muscle disease. The Journal of clinical investigation. 2009; 119:1806–1813. [PubMed: 19587455]
24. Milner DJ, Weitzer G, Tran D, Bradley A, Capetanaki Y. Disruption of muscle architecture and myocardial degeneration in mice lacking desmin. The Journal of cell biology. 1996; 134:1255–1270. [PubMed: 8794866]
25. Li Z, et al. Cardiovascular lesions and skeletal myopathy in mice lacking desmin. Developmental biology. 1996; 175:362–366. [PubMed: 8626040]
26. Psarras S, et al. Regulation of adverse remodelling by osteopontin in a genetic heart failure model. European heart journal. 2010; 33:1954–1963.
27. Milner DJ, Mavroidis M, Weisleder N, Capetanaki Y. Desmin cytoskeleton linked to muscle mitochondrial distribution and respiratory function. The Journal of cell biology. 2000; 150:1283–1298. [PubMed: 10995435]
28. Kuruc N, Franke WW. Transient coexpression of desmin and cytokeratins 8 and 18 in developing myocardial cells of some vertebrate species. Differentiation; research in biological diversity. 1988; 38:177–193. [PubMed: 2463949]
29. Gown AM, Vogel AM. Monoclonal antibodies to human intermediate filament proteins. II. Distribution of filament proteins in normal human tissues. The American journal of pathology. 1984; 114:309–321. [PubMed: 6320650]
30. Ursitti JA, et al. Cloning and characterization of cytokeratins 8 and 19 in adult rat striated muscle. Interaction with the dystrophin glycoprotein complex. The Journal of biological chemistry. 2004; 279:41830–41838. [PubMed: 15247274]
31. Maier HJ, et al. Cardiomyocyte-specific IkappaB kinase (IKK)/NF-kappaB activation induces reversible inflammatory cardiomyopathy and heart failure. Proceedings of the National Academy of Sciences of the United States of America. 2012; 109:11794–11799. [PubMed: 22753500]

32. Brown M, et al. Cardiac-specific blockade of NF-kappaB in cardiac pathophysiology: differences between acute and chronic stimuli in vivo. American journal of physiology. 2005; 289:H466–H476. [PubMed: 15695559]
33. Franke WW, Borrmann CM, Grund C, Pieperhoff S. The area composita of adhering junctions connecting heart muscle cells of vertebrates. I. Molecular definition in intercalated disks of cardiomyocytes by immunoelectron microscopy of desmosomal proteins. European journal of cell biology. 2006; 85:69–82. [PubMed: 16406610]
34. Omary MB, Ku NO, Strnad P, Hanada S. Toward unraveling the complexity of simple epithelial keratins in human disease. The Journal of clinical investigation. 2009; 119:1794–1805. [PubMed: 19587454]
35. Coulombe PA, Omary MB. 'Hard' and 'soft' principles defining the structure, function and regulation of keratin intermediate filaments. Current opinion in cell biology. 2002; 14:110–122. [PubMed: 11792552]
36. Oshima RG. Apoptosis and keratin intermediate filaments. Cell death and differentiation. 2002; 9:486–492. [PubMed: 11973607]
37. Toivola DM, Tao GZ, Habtezion A, Liao J, Omary MB. Cellular integrity plus: organelle-related and protein-targeting functions of intermediate filaments. Trends in cell biology. 2005; 15:608–617. [PubMed: 16202602]
38. Betz RC, et al. Loss-of-function mutations in the keratin 5 gene lead to Dowling-Degos disease. American journal of human genetics. 2006; 78:510–519. [PubMed: 16465624]
39. Kim S, Coulombe PA. Intermediate filament scaffolds fulfill mechanical, organizational, and signaling functions in the cytoplasm. Genes & development. 2007; 21:1581–1597. [PubMed: 17606637]
40. Magin TM, Vijayaraj P, Leube RE. Structural and regulatory functions of keratins. Experimental cell research. 2007; 313:2021–2032. [PubMed: 17434482]
41. Magin TM, et al. Lessons from keratin 18 knockout mice: formation of novel keratin filaments, secondary loss of keratin 7 and accumulation of liver-specific keratin 8-positive aggregates. The Journal of cell biology. 1998; 140:1441–1451. [PubMed: 9508776]
42. Tao GZ, et al. Keratins modulate the shape and function of hepatocyte mitochondria: a mechanism for protection from apoptosis. Journal of cell science. 2009; 122:3851–3855. [PubMed: 19825937]
43. Loranger A, Gilbert S, Brouard JS, Magin TM, Marceau N. Keratin 8 modulation of desmoplakin deposition at desmosomes in hepatocytes. Experimental cell research. 2006; 312:4108–4119. [PubMed: 17126832]
44. Kroger C, et al. Keratins control intercellular adhesion involving PKC-alpha-mediated desmoplakin phosphorylation. The Journal of cell biology. 2013; 201:681–692. [PubMed: 23690176]
45. Green KJ, Gaudry CA. Are desmosomes more than tethers for intermediate filaments? Nature reviews. 2000; 1:208–216.
46. Jamora C, Fuchs E. Intercellular adhesion, signalling and the cytoskeleton. Nature cell biology. 2002; 4:E101–E108. [PubMed: 11944044]
47. Capetanaki Y. Desmin cytoskeleton: a potential regulator of muscle mitochondrial behavior and function. Trends in cardiovascular medicine. 2002; 12:339–348. [PubMed: 12536120]
48. Capetanaki Y, Bloch RJ, Kouloumenta A, Mavroidis M, Psarras S. Muscle intermediate filaments and their links to membranes and membranous organelles. Experimental cell research. 2007; 313:2063–2076. [PubMed: 17509566]
49. Duan S, et al. The Pirh2-keratin 8/18 interaction modulates the cellular distribution of mitochondria and UV-induced apoptosis. Cell death and differentiation. 2009; 16:826–837. [PubMed: 19282868]
50. Fountoulakis M, et al. Alterations in the heart mitochondrial proteome in a desmin null heart failure model. Journal of molecular and cellular cardiology. 2005; 38:461–474. [PubMed: 15733906]
51. Kumemura H, et al. Mutation in keratin 18 induces mitochondrial fragmentation in liver-derived epithelial cells. Biochemical and biophysical research communications. 2008; 367:33–40. [PubMed: 18164256]

52. Stone MR, et al. Absence of keratin 19 in mice causes skeletal myopathy with mitochondrial and sarcolemmal reorganization. Journal of cell science. 2007; 120:3999–4008. [PubMed: 17971417]

53. Molkentin JD, et al. A calcineurin-dependent transcriptional pathway for cardiac hypertrophy. Cell. 1998; 93:215–228. [PubMed: 9568714]

54. Arber S, et al. MLP-deficient mice exhibit a disruption of cardiac cytoarchitectural organization, dilated cardiomyopathy, and heart failure. Cell. 1997; 88:393–403. [PubMed: 9039266]

55. Jahn L, Fouquet B, Rohe K, Franke WW. Cytokeratins in certain endothelial and smooth muscle cells of two taxonomically distant vertebrate species, Xenopus laevis and man. Differentiation; research in biological diversity. 1987; 36:234–254. [PubMed: 2452760]

56. Kaplan SR, et al. Structural and molecular pathology of the heart in Carvajal syndrome. Cardiovascular pathology : the official journal of the Society for Cardiovascular Pathology. 2004; 13:26–32. [PubMed: 14761782]

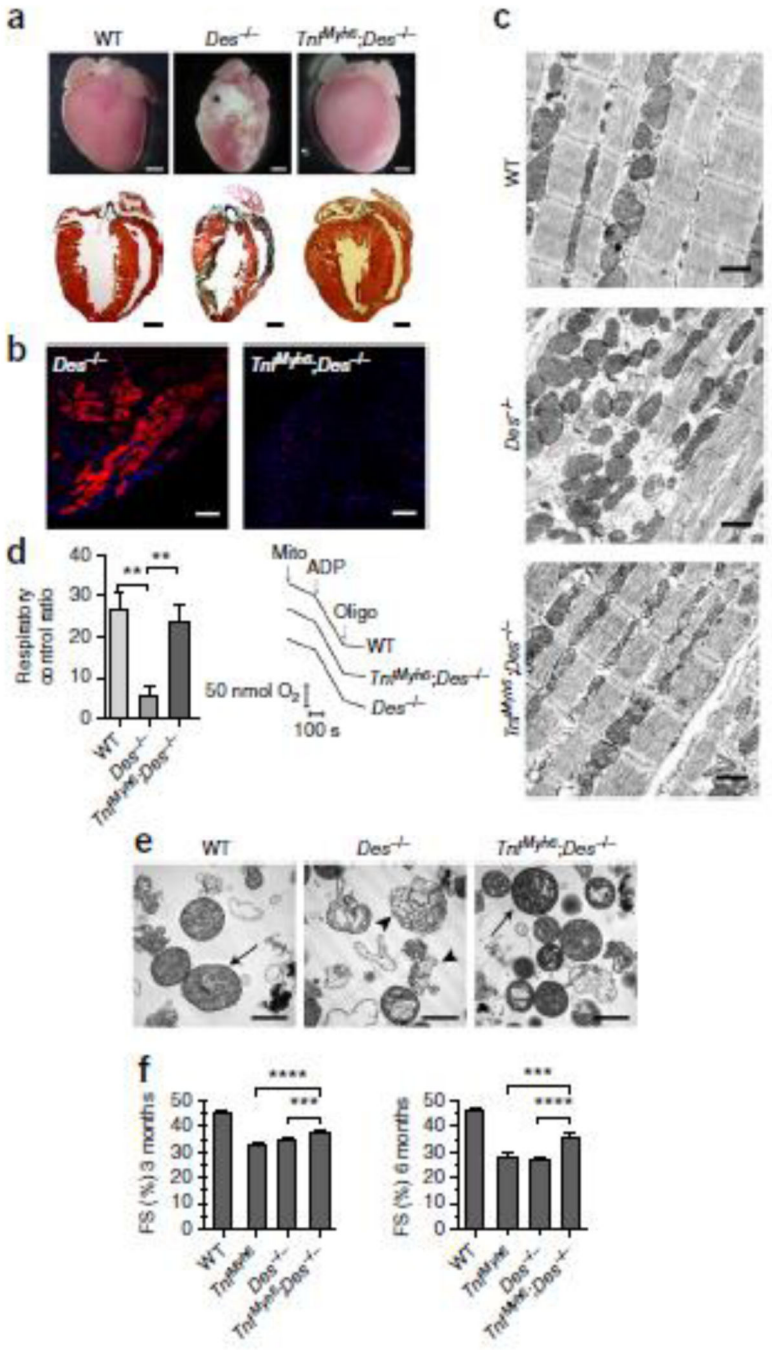

Figure 1. TNF-α overexpression rescues myocardial degeneration, ultrastructural abnormalities, mitochondrial defects and overall cardiac dysfunction caused by desmin deficiency

(**a**) Representative pictures of whole hearts and the corresponding histology by Masson's trichrome staining of cardiac sections of 3-mo-old mice (n=4 mice per genotype). Calcification (white regions) is depicted (asterisk) in Des−/− heart. In histological sections, fibrotic areas with collagen deposition detected in Des−/− hearts are stained in dark green. (**b**) Detection of necrotic areas by Evans Blue Dye (red fluorescence) staining of cryosections of TNFαDes−/− and Des−/− myocardium of 4-mo-old mice. Representative

pictures of n=3 mice per genotype. Scale bars: 100 μm. (**c**) Electron microscopic analysis of the myocardium of 3-mo-old mice (n=3 mice per genotype).. Scale bars: 1 μm. (**d**) Oxygen consumption levels (d´) of isolated cardiac mitochondria from 3-mo-old mice, measured by Clark-type oxygen electrode and presented as respiratory control ratio (RCR; State-III/State-IV) levels. Representative cardiac mitochondrial respiration traces (d´´) of the indicated genotypes. 150 μg of mitochondria (arrow, “mito”) where added to 300 μl EB in presence of 5mM Glutamate - 2.5mM Malate. After 3 min, 400 μM ADP was added (“State-III”) and after 6 min, 1 μM oligomycin (“State-IV”), as indicated by arrows. For sample size, see Supplementary Fig. 5a. (**d**) Transmission electron microscopy of isolated cardiac mitochondria (n=4 mice per genotype). “Class-I” (arrows) and “class-IV” (arrowheads) mitochondria are depicted (as explained in Supplementary Fig. 5),. Scale bars: 1 μm. (**e**) Fractional shortening percentage (FS%) graphs from cardiac function analysis by 2D-directed M-mode echocardiography in 3-mo-old and 6-mo-old mice. For sample size, see Supplementary Table 1. All figure data are presented as mean ± SEM. Two-sided P-value: ** <0.01, *** <0.001, **** <0.0001 (one way ANOVA with Bonferroni/Dunn post-hoc test).

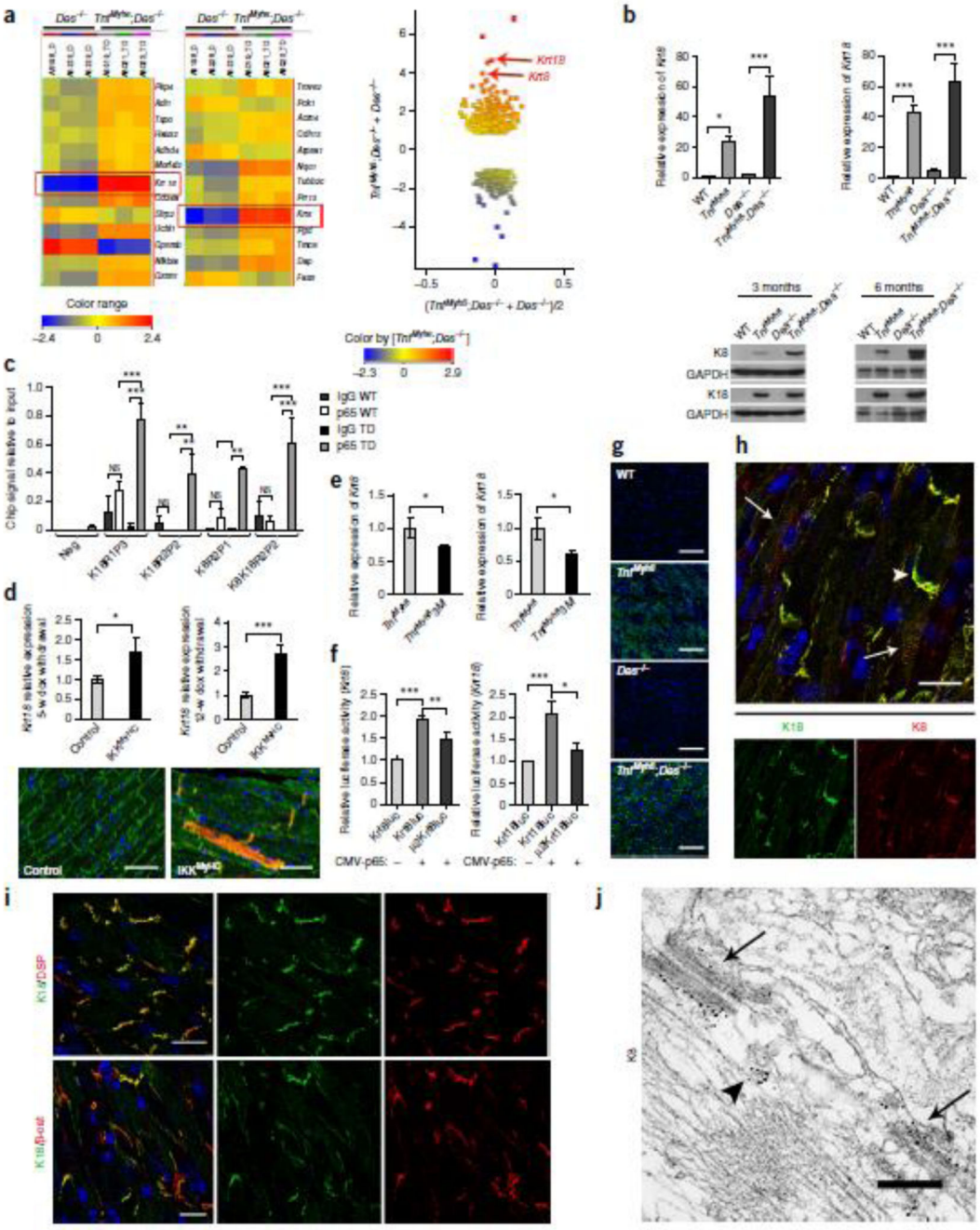

Figure 2. Keratin 8 (K8) and keratin 18 (K18) are ectopically expressed in the TNF-α-overexpressing cardiomyocytes

(**a**) Microarray gene expression analysis comparing TNFαDes−/− versus Des−/− transcriptome (n=3 hearts per genotype, n=3 technical replicates). Heatmap view presenting the hybridization triplicates (a´), and MvA scatter plot (a´´) of all entities (FC≥±2, p-value<0.05), showing *krt8* and *krt18* among the top 3 of the mostly induced genes (a´: red boxes; a´´: red arrows) (Unpaired t-test and Benjamini-Hochberg correction). (**b**) Real-Time PCR analysis of total myocardial RNA for *krt8 and krt18* expression relative to WT (n=6 per

genotype, n=4 technical replicates, one way ANOVA with Bonferroni/Dunn post-hoc test). *Beta-actin* was used as reference gene. (**c**) Western blot analysis for K8 and K18 of total myocardial extracts from 3- and 6-mo-old mice (n=4 mice per genotype). Gapdh levels were used as loading control. (**d**) Chromatin-IP with anti-p65/RelA (n=3 mice per genotype, n=3 biological replicates) followed by RT-PCR analysis. “K18R1P3”, “K18R2P2”, “K8R2P1” and “K8K18R2P2” correspond to regulatory regions of *krt8* and *krt18* loci that showed significant enrichment in ChIPed DNA from TNFαDes−/− (TD) compared to WT hearts (for region analysis see Supplementary Fig. 6). (two way ANOVA with Bonferroni/Dunn post-hoc test). (**e**) Real Time-PCR for *krt18* expression in the myocardium of IKK2^{MyHC} mice with cardiac-specific expression of constitutively active IKK2, 5-weeks and 12-weeks after doxycycline withdrawal relative to their appropriate controls (n=6 minimum per group, n=3 technical replicates, unpaired t-test). *Rpl13* was used as reference gene. (**f**) Immunofluorescence staining for K8 (red) and desmin (green) of cardiac sections of IKK2^{MyHC} and their control mice, 12-weeks after doxycycline withdrawal (n=4 per group). Scale bars: 50 μm. (**g**) Real Time-PCR for *krt8* and *krt18* expression in the myocardium of 6-weeks-old TNFαM3 mice (cross of TNF-α and mice with cardiac-specific expression of IκBα suppersuppressor) relative to their TNF-α littermates (n=11 and n=6 per group, n=3 technical replicates, unpaired t-test). Beta-*actin* was used as reference gene. (**h**) Firefly luciferase reporter activity assays of WT (Krt8luc and Krt18luc) and mutant (μ2Krt8luc and μ2Krt18luc) 2-kb regulatory regions of *krt8* and *krt18*, upon p65 induction. Luciferase activity is presented relative to the respective non-induced WT reporter. All experiments (n=8 minimum) were normalized to β-galactosidase activity (one way ANOVA with Bonferroni/Dunn post-hoc test). (**i**) Confocal laser-scanning immunofluorescence microscopy for K8 (green) expression in cardiac sections of 3-mo-old mice (n=5 mice per genotype). (K18 exhibits similar pattern (not shown).) Scale bars: 100 μm. (**j**) Co-staining for K8 and K18 in TNFαDes−/− (n=5 mice 3-mo-old) myocardium. Co-localization of K8 and K18 at the intercalated disc (arrowhead) and costamere-level (arrows) is presented. Scale bar: 20 μm. (**k**) Co-staining of K18 with desmoplakin (DSP) (k´) and β-catenin (β-cat) (k´´) of cardiac sections from 3-mo-old mice (n=4 mice). Scale bars: 20 μm. (**l**) Electron micrograph of immunogold labeling for keratin 8 (black dots) in TNFαDes−/− cardiac section (n=2 mice, 3-mo-old). ID plaques (arrows) and K8/K18 filaments (arrowhead) are shown. Scale bar: 300 nm. All figure data are presented as mean ± SEM. Two-sided P-values: * <0.05, ** <0.01, *** <0.001.

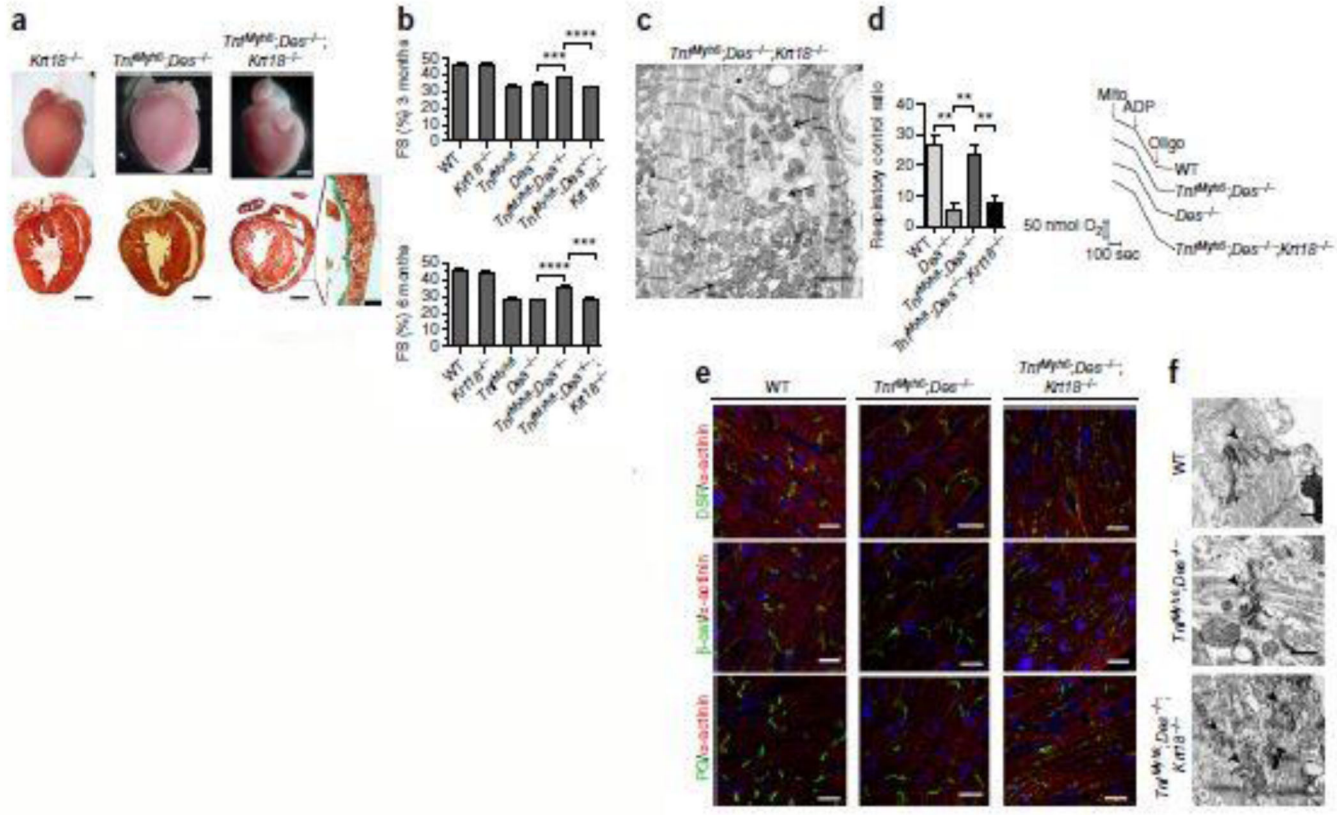

Figure 3. Ectopic expression of K8/K18 confers cardioprotection through maintenance of mitochondrial function and intercalated disc integrity in TNFαDes−/− mice

(**a**) Representative pictures from morphological and histological analysis by Masson's trichrome staining of myocardium from 3-mo-old mice, comparing TNFαDes−/−Krt18−/− with TNFαDes−/− models (n=4 mice per genotype). The myocardium of Krt18−/− control mice presents normal phenotype. Replacement fibrosis of TNFαDes−/−Krt18−/− is depicted in dark green in a´ (enlargement). (**b**) Fractional shortening percentage (FS%) by 2D-directed M-Mode echocardiographic analysis of 3-mo-old and 6-mo-old mice from all groups. For sample size see Supplementary Table 1. The data are presented as mean ± SEM. Two-sided P-values: *** <0.001, **** <0.0001 (one way ANOVA with Bonferroni/Dunn post-hoc test). (**c**) Electron microscopic analysis of TNFαDes−/−Krt18−/− myocardium of 3-mo-old mice (n=2). Severe mitochondrial abnormalities, including fragmentation, disorganization and degeneration (arrows) are shown, together with abnormal organization of myofibrils compared to TNFαDes−/− cardiomyocytes (see Fig. 1c and Supplementary Fig. 3e–f). Scale bar: 2 μm. (**d**) Oxygen consumption levels (d´) of isolated cardiac mitochondria from 3-mo-old mice, measured by Clark-type oxygen electrode and presented as respiratory control ratio (RCR; State-III/State-IV) levels. Representative cardiac mitochondrial respiration traces (d´´) of the indicated genotypes. 150 μg of mitochondria (arrow, "mito") where added to 300 μl EB in presence of 5mM Glutamate - 2.5mM Malate. After 3 min, 400 μM ADP was added ("State-III") and after 6 min, 1 μM oligomycin ("State-IV"), as indicated by arrows. For sample size, see Supplementary Fig. 5a. (**e**) Immunofluorescence microscopy for the ID proteins desmoplakin (DSP), β-catenin (β-cat)

plakoglobin (PG) and with the Z-disc protein α-actinin in cardiac sections of 3-mo-old mice (n=3 mice per group) reveals the mis-localization of the ID proteins and their disrupted pattern in TNFαDes−/−Krt18−/− compared to TNFαDes−/− and WT control cardiomyocytes. Scale bars: 20 μm. (**f**) Electron microscopic analysis comparing the highly abnormal intercalated disc structures (arrowheads) of TNFαDes−/−Krt18−/− compared to that of TNFαDes−/− and control WT cardiomyocytes (n=2 mice of 3-mo-old per genotype). Scale bars: 500 nm.

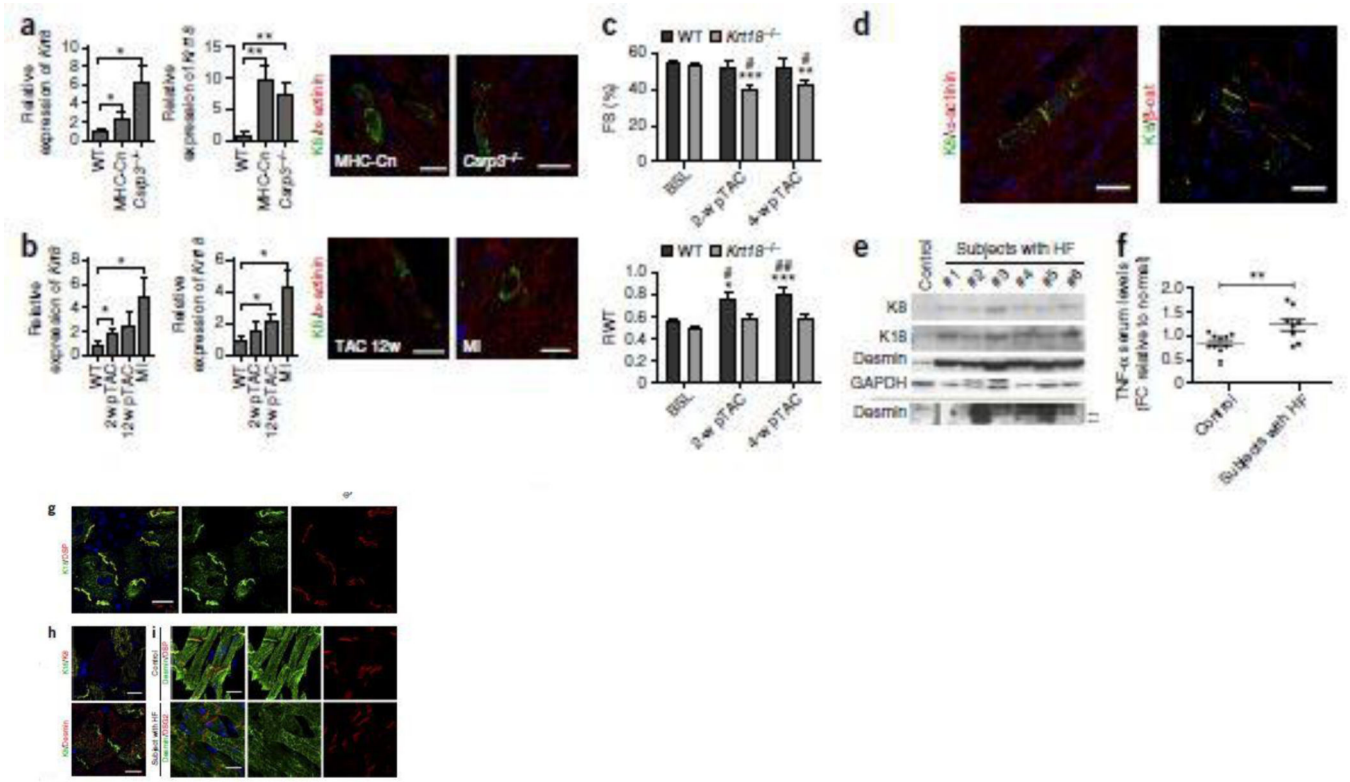

Figure 4. Cardiomyocyte ectopic induction of K8 and K18 is a common response in several genetic and experimental cardiomyopathy models and expands in human heart failure

(**a**) Real-Time PCR (a´) for *krt8* and *krt18* RNA (n=5 at least per group, n=3 technical replicates, unpaired t-test) and immunofluorescence staining for K8 and a-actinin (a´´) (n=2 per group) of the myocardium of 12-weeks-old transgenic mice overexpressing α-MHC promoter-driven active Calcineurin ("**MHC-Cn**") and muscle LIM-protein knockout (**"MLP −/−"**) mice. Expression is presented relative to WT groups. *Rpl13* was used as reference gene. Scale bars: 20 μm. (**b**) Real-Time PCR (b´) for *krt8* and *krt18* RNA (n=5 at least per group, n=3 technical replicates, unpaired t-test) and immunofluorescence staining for K8 and a-actinin (b´´) (n=2 per group) of the myocardium of 8-weeks-old WT C57/BL6 mice, 2-weeks and 12-weeks after transverse aortic constriction ("2-w **pTAC**" and "12-w **pTAC**", respectively) and myocardial infarction by permanent ligation of the left anterior descending (LAD) coronary artery for 4-weeks ("**MI**"). Expression is presented relative to WT groups. *Rpl13* was used as reference gene. Scale bars: 20 μm. (**c**) 2D-directed echocardiographic analysis of fractional shortening (FS) (c´) and relative wall thickness (RWT) (c´´) of 4-months-old WT and krt18−/− mice, before subjected to transverse aortic constriction (TAC) surgery (baseline, "BSL") and 2-weeks and 4-weeks post surgery ("2-w pTAC" and 4-w pTAC" respectively) (for number of animals per group see Supplementary Table 5). Two-sided P-values: * <0.05, ** <0.01, *** <0.001 relative to baseline values, two-sided P-values: # <0.05, ## <0.01 relative to WT (c´) and to Krt18−/− (c´´) group (two way ANOVA with Bonferroni/Dunn post-hoc test). (**d**) Immunofluorescence co-staining for K8, a-actinin and β-catenin of cardiac sections of WT post TAC mice used in Figure 4c, 8-weeks post surgery (n=3). Scale bars: 20 μm. (**e**) Western blot analysis for K8, K18 and desmin of

human end-stage heart failure cardiac samples (n=10 different patients), obtained after transplantation. Representative blots of total cardiac protein extracts from patients #1 – #6 (additional n=4 patient samples are shown in Supplementary Fig. 13a) and control human myocardial sample (n=1 sample of healthy human myocardium) are presented. Arrows at the lower panel show caspase-6-mediated cleavage products of desmin at 24 and 29 kDa. Gapdh levels were used as loading control. (**f**) ELISA for human TNF-α in the serum of the same patients used in the study (n=8). Data are presented as fold change (FC) relative to a normal group (n=10) (unpaired t-test). (**g**) Immunofluorescence microspopic analysis by co-staining for keratin 18 (K18) and desmoplakin (DSP) of human end-stage heart failure cardiac sections (n=3 different patient samples), reveals their co-localization at the IDs. Scale bar: 30 μm. (**h**) Co-staining for K8 with K18 (h´) and K8 with Desmin (h´´) in cardiomyocytes of human patients of end-stage HF (n=3 patients). Scale bars h´: 30 μm; h´´: 20 μm. (**i**) Co-staining of Desmin (DES) and Desmoplakin (DSP) in human myocardial sections of control sample (n=2) (i´). Desmin and Desmoglein-2 (DSG2) co-staining in cardiac sections of patient samples (n=3) (i´´). Notice the loss of desmin from patient IDs (h´´, i´´). Scale bars: 20 μm. Projection images from confocal stacks used at (g–i). All figure data are presented as mean ± SEM. Two-sided P-values: * <0.05, ** <0.01.